Available online at www.sciencedirect.com
ScienceDirect
Journal of Hazardous Materials 151 (2008) 52–57
Journal of Hazardous Materials
www.elsevier.com/locate/jhazmat

A model for computing the trajectories of the conducting particles from waste printed circuit boards in corona electrostatic separators

Jia Li, Hongzhou Lu, Zhenming Xu *, Yaohe Zhou

School of Environmental Science and Engineering, Shanghai Jiao Tong University, 800, Dongchuan Road, Shanghai 200240, People's Republic of China

Received 26 January 2007; received in revised form 14 May 2007; accepted 15 May 2007
Available online 21 May 2007

Abstract

A model for computing the trajectory of conducting particle from waste printed circuit board (PCB) scraps in corona electrostatic separator is established. Using analytical expression for computing non-uniformity of the electric field in the active zone of the separator and the differential method were used for computing the trajectories of conducting particles in the air, after detachment. The result shows that the trajectory of conducting particle can be computed under various initial parameters (R, r, L, α, U, n; ρ, r_0) by the computing model and the computing results have a good agreement with the actual separating process. This model offers a possible for designing the new corona electrostatic separator.

Keywords: Particle trajectory; MATLAB; PCB scraps; Corona electrostatic field

1. Introduction

Corona electrostatic separator (CES) has been investigated extensively in the minerals processing industry. The rotor-type CES, using corona charging, is utilized to separate raw materials into conductivity and non-conductivity fractions [1]. The extreme difference in the density and electrical conductivity between metallic and non-metallic materials provides an excellent condition for the application of the CES in waste printed circuit board (PCB) scraps recycling.

The conducting particles in PCB scraps are mainly metals and they have high value to be recycled [2]. The trajectory of conducting particle depends on particle's characteristic (i.e., dielectric constant), dimension, shape, mass density, as well as on the distribution of electric field strength at the active zone of the CES. Thus, to maximize the utility range of the CES and to guide the effective metal recycling process, a precise computation of the trajectory of the conducting particle from different materials or with different operating parameters of equipments is essential. Many researchers have done large quantity of work on optimizing operating parameters [3–5] and electrostatic field computation [6–8] of the CES. Recently, the study of cylindrical particle trajectories in roll-type corona electrostatic separators had been published [9]. However, the research of trajectories of conducting particles is not thorough enough. Because the value materials in waste PCB were mainly spherical particles (Fig. 6), the aim of the present paper is to establish a model for computing the trajectory of conducting particle in the specific conditions of the CES for recycling value materials from waste PCB.

2. Theoretical aspects

2.1. Physical model and computing flow

The corona electrostatic field of CES is generated by corona electrode and electrostatic electrode in the active zone. The material to be separated is fed by a vibratory feeder onto the rotating roll. The insulating particles are mainly subjected to "ion bombardment" (corona charge) and are "pinned" by the electric image force to the rotating roll, and move with it, finally fall in the holding tanks. While the conducting particles charge in contact with the rotating roll and are attracted to the electrostatic electrode, as shown in Fig. 1.

* Corresponding author. Tel.: +86 21 547 47495; fax: +86 21 547 47495.
E-mail address: zmxu@sjtu.edu.cn (Z. Xu).

0304-3894/$ – see front matter © 2007 Elsevier B.V. All rights reserved.
doi:10.1016/j.jhazmat.2007.05.045

Nomenclature

a	acceleration of the particle (m/s^2)
E	electric field strength (V/m)
F_c	centrifugal force (N)
F_e	electric force (N)
F_g	gravity force (N)
F_i	electric image force (N)
F_r	air drag force (N)
g	acceleration due to gravitation (m/s^2)
L	center distance of rotating roll electrode and electrostatic pole (m)
m	mass of the particle (kg)
n	rotation speed of rotating roll (rev/min)
Q	quantity of electricity (C)
R	radius of the rotating roll (m)
r	radius of the electrostatic electrode (m)
r_0	radius of the particle (m)
U	supplied high-voltage (V)
v	speed of the particle (m/s)
α	included angle of horizontal line and electrodes center line (°)
ε	dielectric constant
η	air drag coefficient (Ns/m^2)
ρ	mass density of the particle (kg/m^3)
ω	angular velocity of rotating roll (rad/s)

A program for computing model was written by MATLAB language. Fig. 2 shows the entire process of computing model:

(1) the non-uniformity electric field strength at the active zone of the CES was computed;
(2) the point where the particle detaches from the rotating roll was computed;
(3) the computed non-uniformity electric field strength in the active zone of the separator was used for computing the particle trajectory in the air, after detachment.

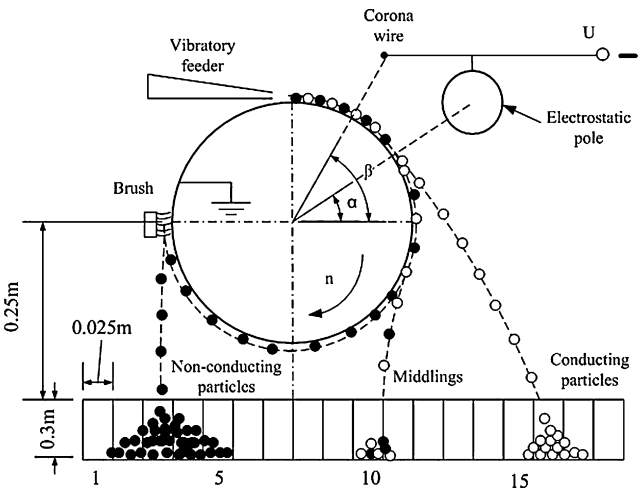

Fig. 1. Diagram of corona electrostatic separator.

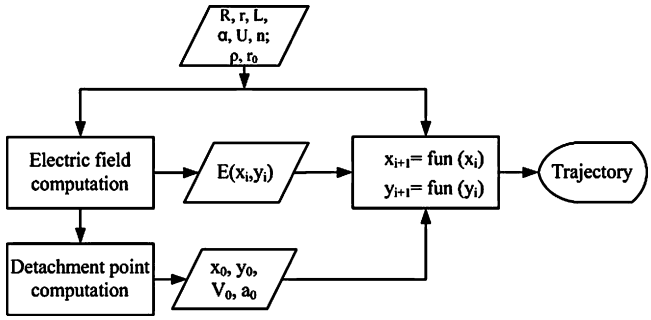

Fig. 2. Flow chart of the program for computing model.

2.2. Field computation

The electrostatic field in the CES was generated by several cylinder electrodes with different diameters. Because the lengths of electrodes are much bigger than their diameters, we consider the electrostatic field has no variation along the axial direction. Then the electrostatic field can be simplified as two-dimensional. Fig. 3 shows the geometric model of electrodes for computing the non-uniformity electric field in the CES. The axis center of rotating roll is considered as the origin of coordinate. The electric field strength (E) in the active zone of the separator is [10]:

$$E_x = \left[\frac{j - h_1 + x_1}{(j - h_1 + x_1)^2 + y_1^2} + \frac{j + h_1 - x_1}{(j + h_1 - x_1)^2 + y_1^2}\right] \times f \tag{1a}$$

$$E_y = \left[\frac{y_1}{(j - h_1 + x_1)^2 + y_1^2} - \frac{y_1}{(j + h_1 - x_1)^2 + y_1^2}\right] \times f \tag{1b}$$

$$E = \sqrt{(E_x)^2 + (E_y)^2} \tag{2}$$

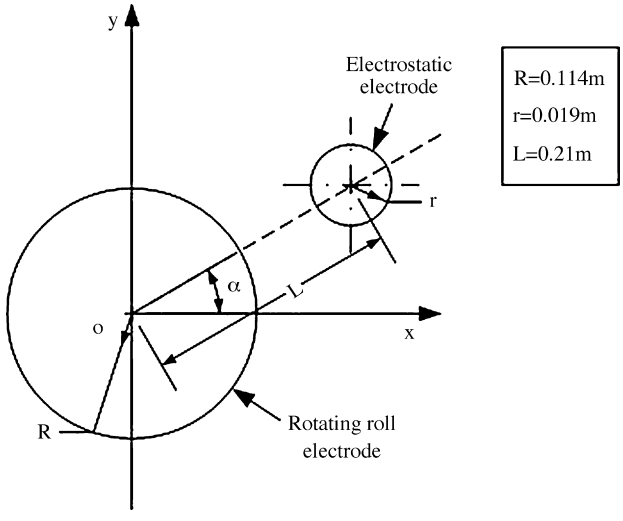

Fig. 3. Geometric model used in electrostatic field computation.

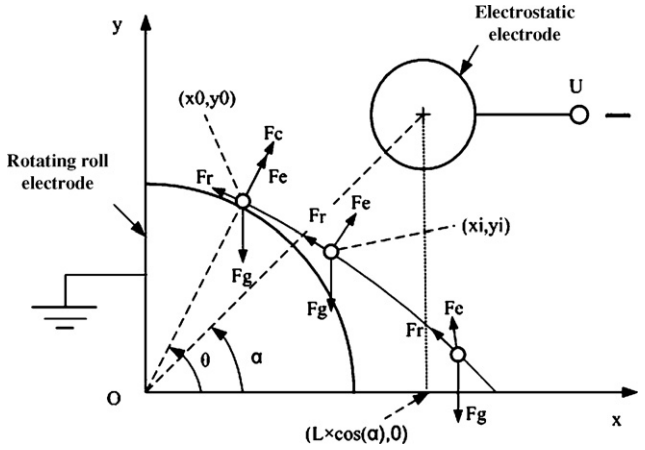

Fig. 4. Geometric configuration for the computation of particle trajectory.

where:

$h_1 = (L^2 + R^2 - r^2) \div (2L);$

$h_2 = (L^2 - R^2 + r^2) \div (2L);$

$x_1 = x\ \cos(\alpha) + y\ \sin(\alpha);$

$y_1 = y\ \cos(\alpha) - x\ \sin(\alpha);$

$j = \sqrt{{h_1}^2 - R^2};$

$$f = U \div \ln \frac{(h_1 + j - R)(h_2 + j - r)}{(R + j - h_1)(r + j - h_2)};$$

U is the supplied high-voltage of electrostatic electrode; E_x and E_y are the horizontal coordinate and vertical coordinate components of the computed electric field strength.

2.3. Detachment points computation

In order to model the particle movement it is assumed that [11]:

(1) the particle is a perfect conducting sphere with radius r_0 and specific mass ρ;
(2) the particle charges instantly through electrostatic induction, at the max value;
(3) the distance between two adjacent particles is very big and each particle can be approximated by a material point;
(4) the space is homogeneous, isotropic with the permittivity ε;
(5) triboelectric charging effects are negligible.

As shown in Fig. 4, before detachment the particle moved with rotating roll at the speed of:

$$v = \omega R \tag{3}$$

where ω is the angular velocity of the rotating roll and R is the radius of the rotating roll.

The particle is detached from rotating roll until the mechanical and electrical forces, which exert on it satisfied the condition (Fig. 4):

$$F_g \times \sin(\theta) = F_e + F_c \tag{4}$$

where $Q = (2/3)\pi^3 \varepsilon r_0^2 E$ is the particle's quantity of charge [12]; $F_g = (4/3)\rho\pi r_0^3 g$ is the gravity force of particle; $F_e = 0.832\text{QE}$ [13] is the electric force; $F_c = (4/3)\rho\pi r_0^3 \omega^2 R$ is the centrifugal force.

Then the particle detaching from rotating roll when:

$$\left(\frac{4}{3}\right)\pi r^3 \rho g \times \sin(\theta) = \left(\frac{4}{3}\right)\pi r^3 \rho\omega^2 R + 17.2\varepsilon r_0^2 E^2 \tag{5}$$

It can be assumed that:

$$z_1 = (4/3)\pi {r_0}^3 \rho g \times \sin(\theta) \tag{6}$$

$$z_2 = (4/3)\pi r_0^3 \rho\omega^2 R + 17.2\varepsilon_0 r_0^2 E^2 \tag{7}$$

Two function curves can be obtained from (6) and (7) and the crossing point of them expresses $z_1 = z_2$, which means the detachment point (θ_d) is confirmed, as shown in Fig. 5. The electric field strength on the surface of rotating roll can be computed from (1a), (1b) and (2) by the replacement of $x_1 = R \times \cos(\theta - \alpha)$ and $y_1 = R \times \sin(\theta - \alpha)$.

2.4. Particle trajectory computation

When the particle detached from rotating roll, the equations of the particle movement in the active zone are (Fig. 4):

When ($x_i < L \times \cos(\alpha)$)

$$\text{ma}_x(x_i, y_i) = F_e(x_i, y_i) + F_r(x_i, y_i) \tag{8}$$

$$\text{ma}_y(x_i, y_i) = F_e(x_i, y_i) + F_r(x_i, y_i) - F_g \tag{9}$$

When ($x_i > L \times \cos(\alpha)$)

$$\text{ma}_x(x_i, y_i) = -F_e(x_i, y_i) + F_r(x_i, y_i) \tag{10}$$

$$\text{ma}_y(x_i, y_i) = F_e(x_i, y_i) + F_r(x_i, y_i) - F_g \tag{11}$$

where $F_{rx} = -6\pi\eta r_0(\text{d}x/\text{d}t)$ and $F_{ry} = -6\pi\eta r_0(\text{d}y/\text{d}t)$ are the Stokes's forces ($\eta = 1.81 \times 10^{-5}\ \text{Nsm}^{-2}$ air drag coefficient); $m = (4/3)\pi r_0^3 \rho$ is the mass of particle.

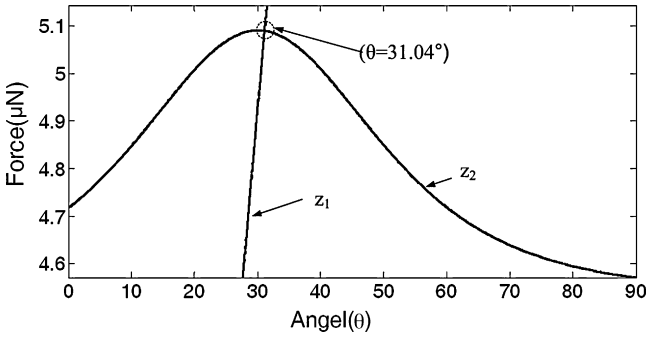

Fig. 5. Graphing method for detachment point computation ($\rho = 8.9 \times 10^3\ \text{kg m}^{-3}$, $r_0 = 0.3$ mm, $n = 60$ rev/min, $U = -25$ KV, $\alpha = 30°$).

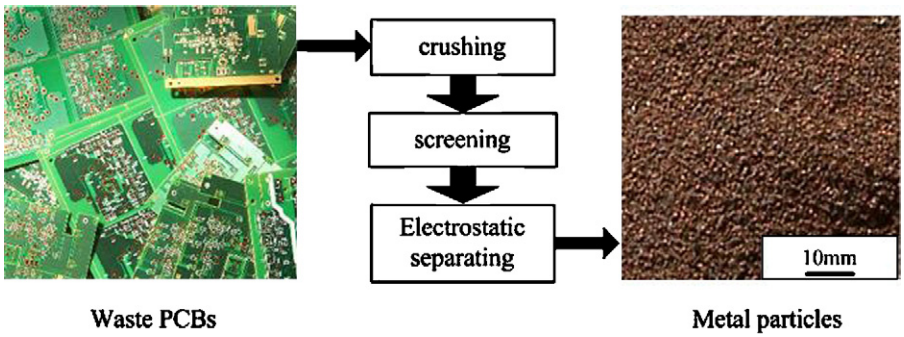

Fig. 6. Flow chart of making conducting particles from waste PCBs.

The F_e changes with particle position; F_r changes with particle speed and F_g is constant. The differential method can most approximately compute the trajectory of the particle. It can be assumed that the particle costs dt to move from (x_i, y_i) to (x_{i+1}, y_{i+1}) with the acceleration $a\,(x_i, y_i)$ and the speed $V\,(x_i, y_i)$ when d$t \to 0$.

The computed detachment point is the first point of trajectory (Fig. 4). The initial speed and acceleration can be computed from (1a), (1b), (2), (6), and (7):

$$V_x(x_0, y_0) = \omega R \sin(\theta_d) \tag{12}$$

$$V_y(x_0, y_0) = \omega R \cos(\theta_d) \tag{13}$$

$$a_x(x_0, y_0) = \frac{[-6\pi\eta V_x(x_0, y_0) + Q_d E_x(x_0, y_0)]}{m} \tag{14}$$

$$a_y(x_0, y_0) = \frac{[6\pi\eta V_y(x_0, y_0) + Q_d E_y(x_0, y_0)]}{m - g} \tag{15}$$

$$x_0 = R \cos(\theta_d) \tag{16}$$

$$y_0 = R \sin(\theta_d) \tag{17}$$

where $Q_d = (2/3)\pi^3 \varepsilon r_0^2 E(x_0, y_0)$ is the particle's charge at the detachment point. Then the position of particle in the air is shown as follows:

$$x_{i+1} = x_i + V_x(x_i, y_i)\mathrm{d}t + 0.5a_x(x_i, y_i)\mathrm{d}t^2 \tag{18}$$

$$y_{i+1} = y_i + V_y(x_i, y_i)\mathrm{d}t + 0.5a_y(x_i, y_i)\mathrm{d}t^2 \tag{19}$$

where:

$$V_x(x_i, y_i) = V_x(x_{i-1}, y_{i-1}) + a_x(x_{i-1}, y_{i-1})\mathrm{d}t \tag{20}$$

$$V_y(x_i, y_i) = V_y(x_{i-1}, y_{i-1}) + a_y(x_{i-1}, y_{i-1})\mathrm{d}t \tag{21}$$

$$a_y(x_i, y_i) = \frac{[6\pi\eta V_y(x_{i-1}, y_{i-1}) + Q_d E_y(x_{i-1}, y_{i-1})]}{m - g} \tag{22}$$

When the particle flying to the position with the same horizontal coordinate, the direction of F_e changed (Figs. 4 and 8), then the equations will be:

When $x_i < L \times \cos(\alpha)$

$$a_x(x_i, y_i) = \frac{[-6\pi\eta V_x(x_{i-1}, y_{i-1}) + Q_d E_x(x_{i-1}, y_{i-1})]}{m} \tag{23}$$

When $x_i > L \times \cos(\alpha)$

$$a_x(x_i, y_i) = \frac{[-6\pi\eta V_x(x_{i-1}, y_{i-1}) - Q_d E_x(x_{i-1}, y_{i-1})]}{m} \tag{24}$$

The MATLAB language is used to program software, which can make calculation speed faster, calculated precision higher and protracting figure easier. On the basis of (12. . .24), a program written by MATLAB language is used (Fig. 2) to compute and plot the trajectory of conducting particle; the time step (dt) is set at 0.1 ms. The operating parameters of CES (R, r, L, α, U, n) and the characteristic of particle (ρ, r_0) are input data for the program. Variation of input data can plot different trajectories (Fig. 10).

3. Experiment materials and methods

The conducting particles used in this study were collected from scraps of a local PCBs factory (without electronic elements). Through the pre-processing, the average size of conducting particles was +0.6–0.8 mm, as shown in Fig. 6. The CES used in this study was laboratory rotor-type, as shown in Fig. 1. The operating parameters of separator matched the geometric model (Fig. 3). The conducting particles fed on the surface of the rotating roll with an electric vibratory feeder. A digital camera was used to capture the moment of the particle detaching from

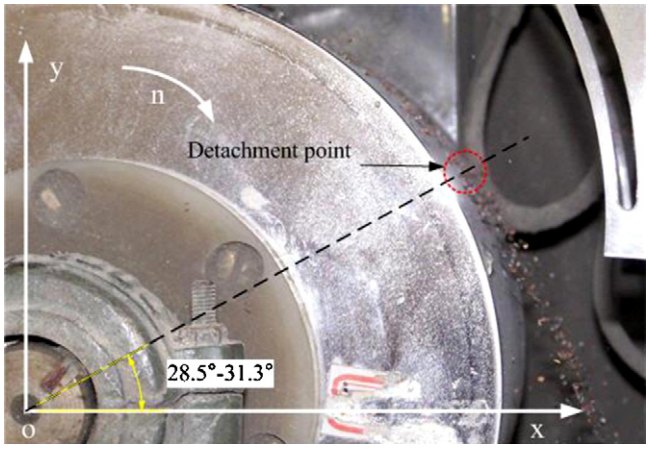

Fig. 7. Photograph of conducting particles detaching from rotating roll ($\rho = 8.9 \times 10^3$ kg m^{-3}, $r_{0\,min} = 0.3$ mm, $r_{0\,max} = 0.4$ mm, $n = 60$ rev/min, $U = -25$ KV, $\alpha = 30°$).

the rotating roll. There are eighteen holding tanks for collecting particles (Fig. 1).

4. Results and discussion

As shown in Fig. 5, the function curves (z_1 and z_2) are made with Cu particle since it is the main metal component in PCB scraps and the detachment points are $\theta_d = 31.04°$($r_0 = 0.3$ mm) and $\theta_d = 30.10°$($r_0 = 0.4$ mm). Fig. 7 shows the experimental results with the conducting particles from PCB scraps and their detachment points were $\theta_{d\,min} = 28.5°$ and $\theta_{d\,max} = 31.3°$. The results show a good agreement between the computed and measured values of the θ_d.

The analytical expression of the electric field used in this study was for single electrostatic electrode structure. However, we use composite electrodes (single electrostatic electrode and single corona electrode) in the experiment, as shown in Fig. 1. The partial differential equation (PDE) toolbox, which, provides a powerful and flexible environment for the study and solution of partial differential equations in two space dimensions and time in MATLAB 7.0 was a convenient and fast tool to simulate electrostatic field in corona electrostatic separator. As shown in Fig. 8, the distribution of electric field strength on the surface of rotating roll was simulated by the PDE toolboxes and the variation of the electrostatic field as function of the angle was shown in Fig. 9. As discussed previously, the detachment points were mainly less than 32° in experiments. When the angle was less than 32°, the values of electric field strength distribution between single and composite electrode structures were so close (Fig. 9) that the influence of the corona electrode can be neglect during the computation.

Fig. 10 shows the trajectories plotted by the program and the horizontal positions of particles on the holding tanks for different rotation speeds of rotating roll. The positions of the particles fall into the holding tanks are measured, as presented in Table 1. The motion of particles falling from detachment point to the holding tanks costs about 0.2 s. The results computed by the model have a good agreement with the experimental results (Table 1). The impact of rotation speed to the particle trajectories was seen directly and clearly by the computing model results (Fig. 10).

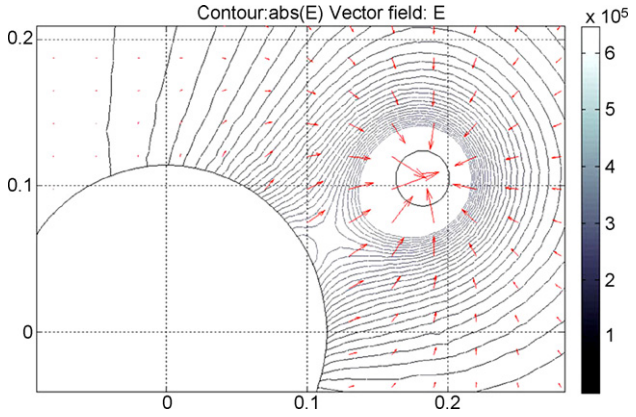

Fig. 8. Diagram of simulation distribution of electrostatic field in the separator with MATLAB 7.0 (10 KV m^{-1} ~ 300 KV m^{-1}), the boundary condition is Dirichlet condition. ($U = -25$ KV, $\alpha = 30°$, $r = 0.019$ m, $L = 0.21$ m).

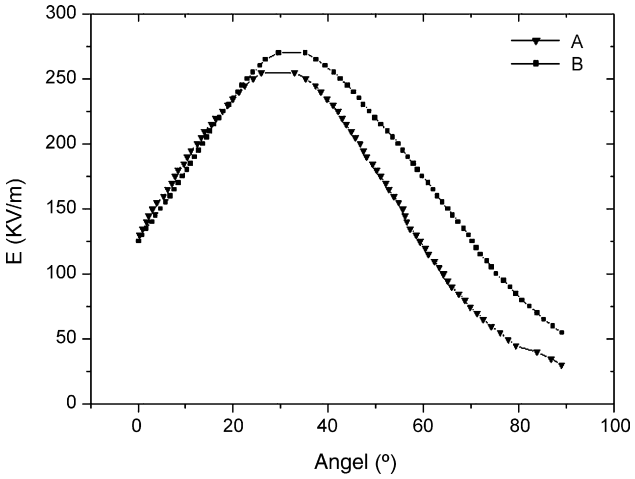

Fig. 9. Electric-field strength distributions on the rotating roll under different electrode structures, (A) single electrostatic electrode $\alpha = 30°$, (B) single electrostatic electrode $\alpha = 30°$ + single corona electrode $\beta = 60°$. ($U = -25$ KV).

All the initial parameters (R, r, L, α, U, n; ρ, r_0) can be changed by the model. The parameters of "R, r, L and α" present the electrode structures and "U, n" present the input operating parameters of CES. During the experiments and manufacturing, frequent replacement of electrodes and operating parameters to achieve the best separating results wasted time and money. Using the model can solve these problems. Through computing the trajectories of particles with different ρ, it is possible that a new separator can be used to separate different metals such as copper and alumina.

After detachment, the trajectory of particle is determined by F_e, F_r and F_g (Fig. 4). As shown in Fig. 11, F_g is much bigger than F_e and F_r when the size of particles is large. But the small particle is subjected to more impact of F_e and F_r. The trajectory

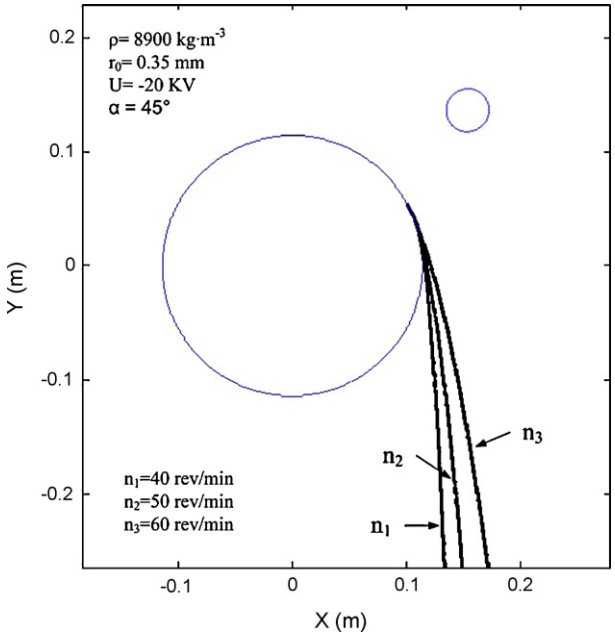

Fig. 10. Diagram of computed trajectories of conducting particles for different rotational speeds ($R = 0.114$ m, $r = 0.019$ m, $L = 0.21$ m).

Table 1
The detachment angle θ_d and horizontal positions ($y = -0.25$ m) for different rotational speeds

n (rev/min)	θ_d (°)	Time cost (s)	Computing value X (m)	Weight contents (%) of collecting boxes				
				11	12	13	14	15
40	12.3	0.1924	0.132	10	83	6	1	0
50	19.4	0.1902	0.147	5	78	13	4	0
60	28.7	0.1918	0.169	0	4	85	9	2

($\rho = 8.9 \times 10^3$ kg m^{-3}, $r_{0\,min} = 0.3$ mm, $r_{0\,max} = 0.4$ mm, $n = 60$ rev/min, $U = 20$ KV, $\alpha = 45°$).

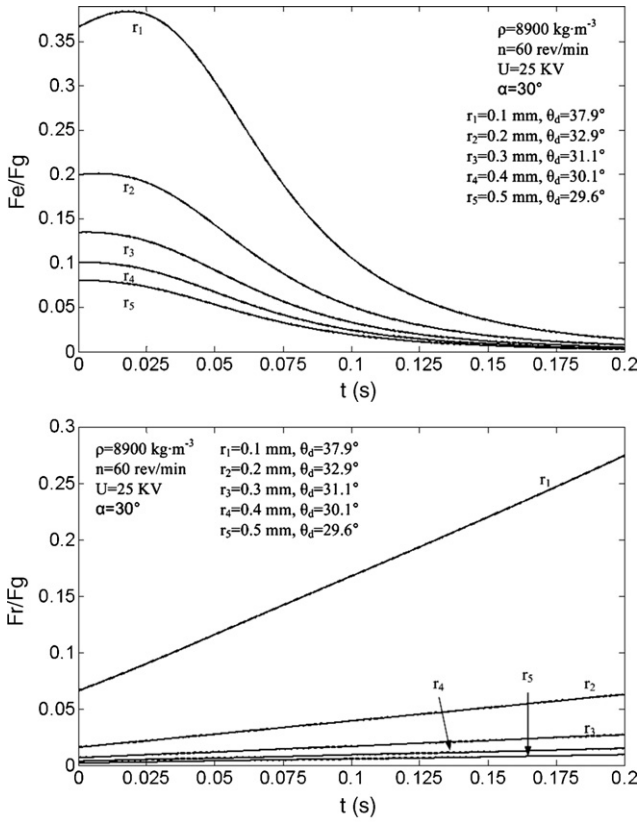

Fig. 11. Forces exerting on the particles for different radius after detachment.

of the large particle is similar to oblique parabolic orbit and the initial conditions of particle flight (detachment point) have more impact on the trajectory of large particle than the trajectory of small particle.

5. Conclusions

A model for computing the trajectory of conducting particle in the specific conditions of the corona electrostatic separator is established. The trajectory of conducting particle computed by the model has a good agreement with the actual separating process.

The trajectory of large particle is similar to oblique parabolic orbit and the initial conditions of particle flight (detachment point) have more impact on the trajectory of large particle than small particle.

This model can also be used to analyze the influence of various operating parameters and particles characteristic on trajectory of conducting particle.

Acknowledgments

This project was supported by the National High Technology Research and Development Program of China (863 program 2006AA06Z364), Program for New Century Excellent Talents in University and the Research Fund for the Doctoral Program of Higher Education (200060248058).

References

[1] J. Cui, E. Forssberg, Mechanical recycling of waste electric and electronic equipment: a review, J. Hazard. Mater. B99 (2003) 243–263.
[2] ehner Theo. Integrated recycling of non-ferrous metal at Boliden Ltd. IEEE International Symposium on Electronics & the Environment (1998) 42–47.
[3] A. Iuga, V. Neamtu, I. Suarasam, R. Morar, L. Dascalescu, Optimal high-voltage energization of corona-electrostatic separators, IEEE Trans. Ind. Appl. 34 (1998) 286–293.
[4] R. Morar, Al. Iuga, L. dascalescu, A. Samuila, Factors which influence the insulation–metal electroseparation, J. Electrostat. 30 (1993) 403–412.
[5] Lucian Dascalescu, Amar tilmatine, Florian Aman, and Michaela Mihailescu, Optimization of electrostatic separation processes using response surface modeling, IEEE Trans. Ind. Appl., Vol. 40, No. 1, January/February 28.
[6] D. Rafiroiu, C. Munteanu, R. Morar, A. Meroth, P. Atten, L. Dascalescu, Computation of the electric field in wire electrode arrangements for electrostatic processes applications, J. Electrostat. 51–52 (23) 571–577.
[7] Dan Rafiroiu, Ilie Suarasan, Roman Morar, Pierre Atten, Lucian Dascalescu, Corona inception in typical electrode configurations for electrostatic processes applications, IEEE Trans. Ind. Appl., Vol. 37, No. 3, May/June 23.
[8] L. Dascalescu, Mouvements des particules conductrices dans un séparateur à haute tension pour matériaux granulaires, J. Electrostat. 32 (1994) 305–316.
[9] M. Younes, A. Tilmatine, K. Medles, M. Rahli, L. Dascalescu, Numerical modelling of conductive particle trajectories in roll-type electrostatic separators, Conference Recordings of IEEE/IAS Annual Meeting, Hong Kong, 2005, pp. 2601–2606.
[10] Ангелов А И, Верещагин И П, Ершов В С, и др Физические основы элктрической сепарации [M]. Москва Недра, 1983: 160.
[11] Simona Vlad, Alin Urs, Alexandru Iuga, Lucian Dascalescu, Premise for the numerical computation of conducting particle trajectories in plate-type electrostatic separators, J. Electrostat. 51–52 (23) 259–265.
[12] Simona Vlad, Michaela Mihailescu, Dan Rafiroiu, Alexandru Iuga, Lucian Dascalescu, Numerical analysis of the electric field in plate-type electrostatic separators, J. Electrostat. 48 (21) 217–229.
[13] N.J. Félici, Forces et charges de petitis objets en contact avec une électrode affectée d'un champ électrique, Rev. Gen. Elect. 75 (1966) 1145–1160.